

Palm Reading: Using Palm Deformation for Fingers and Thumb Pose Estimation

Mohammad Fattahi Sani, Mario Esteban Ochoa, Sanja Dogramadzi

Abstract—Hand pose estimation is recognised as being one of the most challenging topics in the field of human pose estimation. Accurate estimation and tracking of multi degree of freedom hand joints can be beneficial to many research areas such as robotic tele-manipulation, motion patterns, robotic hand design and, more generally, human computer/robot interaction. Current solutions to hand tracking are unsatisfactory due to numerous simplifications used in modeling of the hand kinematics and noise-prone hand and finger position sensing methods. In this paper, we propose alternative hand pose sensing approach that includes detecting palm shape in order to more accurately estimate joint angles of middle and index fingers and thumb. We use Inertia Measurement Unit (IMU) sensors on the palm to detect forming of palm arches in different fingers and thumbs' poses. Principal component analysis as well as Dynamic Neural Networks are utilized to create three different models for fingers and thumb poses, while Polaris optical motion capture system is used as a ground truth. Validating through the unused data shows that using the palm shape as an additional parameter in hand tracking can estimate the hand digit joint angles with the average error of under 4.1%.

Index Terms—Finger tracking tracking, Palm Shape, Machine Learning, neural networks.

I. INTRODUCTION

Human hand is by far one of the most sophisticated tools in nature. Thanks to its intricate mechanisms, we are capable of creating a variety of power and precision grasps necessary to interact with our environment [1]. Understanding the mechanisms behind this variety of movements is of paramount importance in many applications such as healthcare engineering, rehabilitation, ergonomics, education, entertainment and robotics, among others. Precise and accurate hand motion tracking is undoubtedly a prerequisite for better understanding of human hand kinematics and grasp recognition.

Most hand modelling approaches consider the hand as a mechanism formed by independent rigid bodies connected to the palm, which represents an extra rigid link [2]. The palm itself is a flexible body comprised of a set of connected rigid bodies [3] and has a crucial role in finger and thumb motion. The current literature does not consider a potential of detecting palm to improve accuracy of hand tracking.

This paper describes the development related to detecting a palm shape to improve accuracy of tracking hand digits. We propose a model based on Dynamic Neural Network (DNN) for accurate finger and thumb motion tracking which also takes

*This research is supported by SMARTSurg project, funded by the European Unions Horizon 2020 research and innovation programme under grant agreement No 732515.

All authors are with Bristol Robotics Laboratory(BRL), Coldharbour Lane, Bristol, UK. Email: Sanja.Dogramadzi@brl.ac.uk

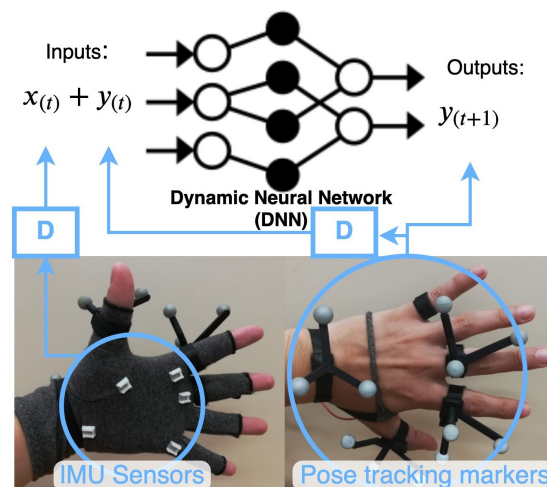


Fig. 1. Proposed Sensing Network. (left: IMU sensors on the palm, right: Reflective-IR markers on the fingers used as a ground truth).

* Inputs are one step delayed compared to the outputs

palm deformation into account. We use IMU sensors placed on the palm and the fingers' and thumb's phalanges to estimate more accurately the digits' pose. Figure 1 shows a conceptual overview of the proposed architecture.

II. RELATED WORK

A growing body of literature has investigated human pose estimation for variety of purposes ranging from human computer interfaces and medical applications to security use cases [4]. Technologies for pose estimation can be classified in vision-based [5] and wearable motion capture systems [6]. A recent survey of using computer vision methods for hand pose estimation can be found in [7]. Wearable technologies for hand tracking span from mechatronics devices that convert motion into electrical signals to small sensors that can fit on the hand. Their typical shortcomings include a lack of adjustment to different hand sizes, difficulties in aligning mechanisms to hand joint axis and movement of the sensors attached to the skin. Vision-based methods, although having the benefit of being non-contact, suffer from occlusions and noise [7].

Various neural network architectures have been suggested for motion estimation and prediction such as general regression neural network (GRNN) [8], adaptable neural networks [9], deep learning [10], and recurrent neural networks [11].

Hand pose estimation, which includes fingers, thumb, and wrist motion tracking, has numerous applications in the field of patient motion analysis, virtual reality, tele-operation of

robotic master slave systems, and surgical robotics [4], to name the few. In synergy based tele-operation applications, for instance, reliable estimation of the finger, thumb and wrist joint angles play a key role in success of operation. However, the hand's complex structure and articulation make its pose estimation more challenging compared to the whole body pose estimation [10].

A wide range of commercially available hand tracking devices have been designed for gaming and virtual reality [12]. These devices utilise various soft resistive sensors or IMUs with the rotational accuracy of up to 0.01 degrees [13], while some also integrate haptic feedback [14]. However, accurate estimation of hand joints, particularly in the thumb are still an open issue.

In the literature, only a few studies considered palm shapes in relation to hand kinematics. A bio-mechanical analysis of the inner palm arches related to two power grasps (spherical and cylindrical) as well as other factors that change the shape of the hand such as the grasped object size and the location of an object in the hand was performed by [15].

In another study [16], the authors recognised the importance of the palm degrees of freedom when designing hand rehabilitation exoskeletons. They analyzed the role of the palm in a series of activities of daily living and subsequently designed a hand exoskeleton with active thumb joints which allows complex hand shaping. The movements exerted by this exoskeleton help the user to create palm arches that can not be supported by most exoskeletons that only actuate hand digits.

Tracking palm is particularly interesting for gesture recognition. In [17], the authors used photo-reflective sensors and a Leap Motion sensor to detect deformations of the dorsal side of the palm. Support Vector Machine (SVM) algorithm was used for collected data classification with 99.5% accuracy. Similarly, [18] used an RGB camera and a depth camera to estimate gestures based on palm and finger shapes while interacting with objects in virtual environments.

Palm shape was also explored as a biometric recognition feature [19] using a depth camera (Kinect) and a machine learning algorithm to classify the collected hand features. A similar classification task, only with additional geometric palm parameters - perimeter and convex area of the palm, was performed by [20]. The aim of the research was to identify a surgeon in the operating room just from his/her palm shape. Additional palm features such as depth of palm centre, horizontal cross-sectional area and a radial line length over the palm shape were similarly utilized by [21] to identify a person from the 3D shape of the palm.

Although considerable research in hand/finger tracking have been reported, a palm shape has so far not been used as an additional source of data for improving hand tracking accuracy. Given the lack of research in this direction, the main contribution of this paper includes:

- an optimized sensing architecture for palm shape detection
- a test-bed for collecting high quality thumb, finger and palm pose data sets

TABLE I
DEGREES OF FREEDOM OF EACH JOINT IN THE THUMB, MIDDLE AND INDEX FINGER

Digits	Type of joint	DOFs
Index, Middle, Ring, Little	Distal Interphalangeal (DIP)	1
	Proximal Interphalangeal (PIP)	1
	Metacarpophalangeal (MCP)	2
Thumb	Interphalangeal (IP)	1
	Metacarpophalangeal (MCP)	1
	Carpometacarpal (CMC)	3

- finger and thumb pose estimation using dynamic neural networks and Principal Component Analysis (PCA)
- evaluation of the proposed tracking method using Northern Digital Inc.(NDI)'s Polaris motion capture system.

III. HAND AND PALM KINEMATICS

The dexterity of a human hand is, to a great extent, caused by the complex structure of its bones, muscles and tendons. However, to avoid extra complexity, only the skeletal structure of the hand is considered for this study. The skeletal parts of the human hand and related abbreviations are shown in table I [22].

In this work we utilized a skeletal kinematic model which models phalanges as rigid links and finger and thumb joints as joints of the kinematic chain with different degrees of freedom Degrees of Freedom (DOF). From previous studies we know that fingers and thumb have 21 DOFs. Due to the opposable nature of the thumb, 5 of 21 DOFs are produced by the thumb, and 4 DOFs by each finger [23]–[25]. See Table I for DOF of each joint of fingers and thumb.

Consequently, human hand can be difficult to model requiring multiple sensing points to track 21 DOFs independently. However, the DOFs can be reduced due to the fact that some fingers typically move together, either because the central nervous system simplifies their control by actuating several joints at the same time, or certain tendons move more than one finger at the time. This allows reduction of the model and tracking complexity [26].

Hand palm, according to Ref. [15], can form 3 different arches defined as Distal transverse, formed by the MCP of the little, ring, middle and index fingers; Longitudinal, from the MCP of the middle finger to the crease of the wrist; and, Oblique, that is the concave curvature formed between the thumb and the other 4 fingers (See Figure 2).

The arches are used to model an estimator of palm shape which consequently predicts finger and thumb joint angles. It is worth mentioning that palm arches are analyzed independently and the relation between them goes beyond the scope of this paper.

IV. METHODOLOGY

In this section, the proposed data acquisition methodology is explained for ground truth data collection as well as IMU data collection. In addition, a neural network model is suggested to estimate the finger joint angles given the collected data.

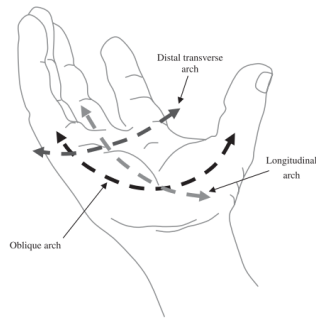


Fig. 2. "Arches of the hand: distal transverse, longitudinal and oblique" [15]

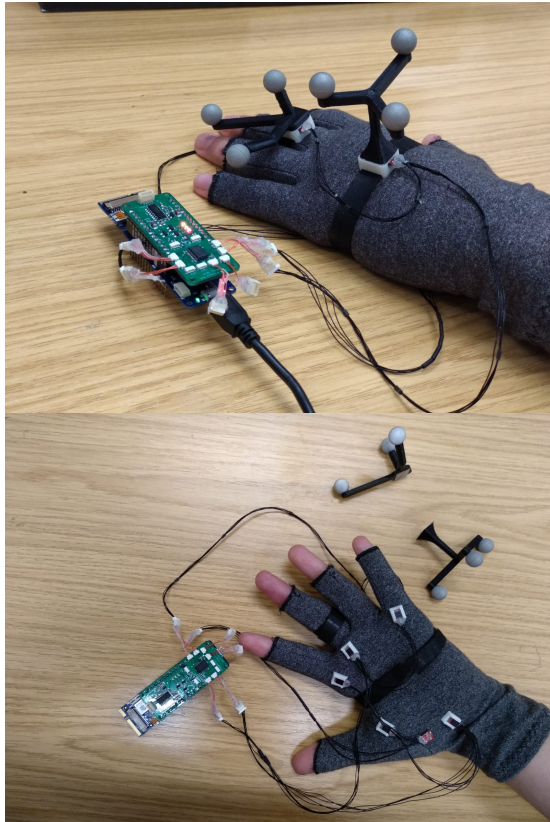


Fig. 3. (Top) IMU sensors and Ground truth markers location (Middle finger). (Bottom) Palm IMU sensors location

The absolute orientation of the links and palm shape recorded by IMUs are used to estimate MCP joint angle of the middle and index fingers, and the CMC joint of the thumb. Reference values of these angles are acquired by a motion capture system (Polaris, NDI). Fig. 3 illustrates our experimental setup including the bespoke 3D printed tools for Polaris markers and 3D printed IMU sensor holders.

A. Ground Truth using Polaris motion capture system

For a global 3D orientation of the palm, fingers and thumb, a specific set of tools for Polaris reflective infrared markers has been designed and attached to the fingers, thumb and palm (see Fig. 1). Polaris Spectra [27] motion capture system

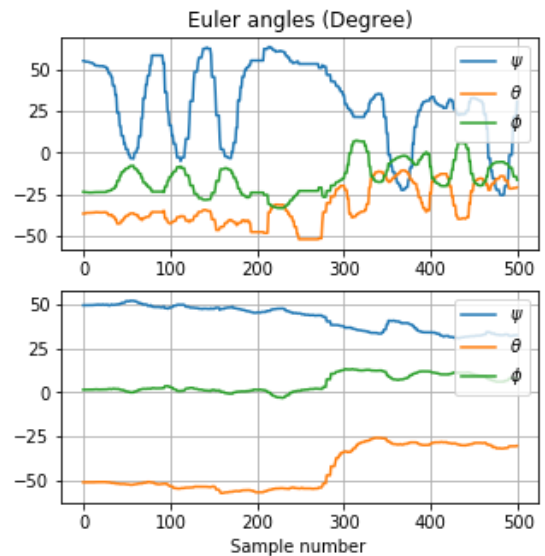


Fig. 4. Absolute orientation of the Index finger (Top), and Palm (Bottom) recorded by Polaris

tracks the markers in 6-DOF and acquires their pose using a proprietary 'NDI track' software. The pose data captured using sawNDITracker library from Computer-Integrated Surgical Systems and Technology (CISST) [28] are published in Robot Operating System (ROS). Assuming P_f^C and P_p^C as poses of the three hand digits and the palm in the camera frame, respectively, P_f represents a finger or thumb pose with respect to the palm. Fig. 4 shows sample data of the index finger movements.

B. IMU sensor data collection

Five BNO0555 IMU sensors from Bosch [29] are placed on the three digit phalanges and the palm. A custom data acquisition board is designed with an ARM Cortex-M0 processor equipped with an 8-channel I2C switch, PCA9548A [30]. Orientation data acquired by the IMU sensors are sent to a PC running ROS on Ubuntu 16.04. Specific ROS nodes are parsing messages coming from the data acquisition board and publishing them as time stamped ROS topics, performing frame transfers, and synchronizing all the messages from Polaris and IMUs. Polaris tracks the markers at the rate of 50Hz, and the IMU sensor board samples the data at 100Hz. Orientations of the hand digits and the palm are represented as quaternions since this is a more consistent way than using Euler angles which suffer from Gimbal lock problem and discontinuity when crossing π values. Assuming $q = [q_x, q_y, q_z, q_w]$ as a quaternion value, q_r describes a relative quaternion for each joint.

1) *Sensor location*: Location of the sensors in our experiments are as follows:

1) Middle finger angle estimation

- Polaris markers over the MC and the PP of the middle finger
- IMU over the MC and the PP of the middle finger

- IMU over the pivot points of the longitudinal arch
- 2) **Index finger** angle estimation
- Polaris markers over the MC and the PP of the index finger
 - IMU over the MC and the PP of the index finger
 - IMU over the distal palmar part of the MC bone of the index finger
 - IMU over the palmar part of the wrist
- 3) **Thumb** angle estimation
- Polaris markers over the wrist and the MC of the thumb
 - IMU over the wrist and the MC of the thumb
 - IMU over the distal palmar part of the MC bone of the thumb
 - IMU over the palmar part of the wrist

Two data sets of approximately 2500 samples for each finger and the thumb have been collected and split into two data sets for training and testing.

- In the first stage (**exp. 1**), the MCP joint angles of the middle and index fingers are estimated using the measurements of the absolute orientation of the MC and PP links (Figure 3a). For the thumb, the CMC joints angles are estimated using the wrist and the MC link absolute orientation. They are measured by IMU sensors located over the mentioned links.
- In the second stage (**exp. 2**), the same angles are measured using the palm shape information acquired by IMU sensors placed over the palm surface as shown in Figure 3.
- In the third stage (**exp. 3, 3A, and 3B**), the first and second stage estimated data are combined.

C. Comparison of Neural Network models

Two different neural network architectures with different number of layers were assessed for accuracy:

- **A1:** Feedforward Neural Network for each dimension of data (roll, pitch, yaw), 1 input layer, 1 sigmoid hidden layer with N neurons, and 1 linear output layer with 1 output.
- **A2:** Feedforward Neural Network for all dimensions of data (roll, pitch, yaw), 1 input layer, 1 sigmoid hidden layer with N neurons, and 1 linear output layer with 3 outputs.
- **A3:** Dynamic Neural Network (Nonlinear Autoregressive with External input) for all dimensions of data (roll, pitch, yaw), 1 input layer, 1 sigmoid hidden layer with N neurons, 2 delays, and 1 linear output layer with with 3 outputs.

A1, A2, and A3 architectures with 5 different configurations are trained and tested with a collection of 5 datasets of the random motion of 3 digits. At this stage, we explored appropriateness of models with different number of inputs and outputs. All the above architectures are trained with the Bayesian Regularization back-propagation algorithm. With 70% of the dataset for training, 10% for validation and 20%

TABLE II
COMPARISON OF MSE ERROR OF 3 DIFFERENT ARCHITECTURES (A1, A2, A3), WITH 5 DIFFERENT CONFIGURATIONS (A, B, C, D, E) FOR MIDDLE FINGER, INDEX FINGER AND THUMB

Middle Finger				
ID	Neurons	A1 MSE	A2 MSE	A3 MSE
a	2	13.48%	13.60%	9.82%
b	3	13.61%	13.84%	10.45%
c	4	13.75%	13.50%	11.48%
d	5	13.94%	13.77%	11.72%
e	10	13.48%	13.73%	19.37%
Index Finger				
ID	N	A1 MSE	A2 MSE	A3 MSE
a	2	4.83%	4.81%	3.45%
b	3	4.83%	4.81%	3.37%
c	4	4.84%	4.81%	3.36%
d	5	4.85%	4.84%	3.96%
e	10	4.88%	4.86%	8.59%
Thumb				
ID	N	A1 MSE	A2 MSE	A3 MSE
a	2	47.81%	48.15%	20.54%
b	3	46.65%	47.20%	20.97%
c	4	48.81%	52.04%	23.67%
d	5	49.08%	50.38%	39.95%
e	10	48.84%	51.15%	55.84%

for testing. Comparison of the mean square error of the 3 models with the ground truth is shown for the index finger in Table II.

Table II shows that the last model (A3) has the most optimal accuracy. We have used the same modelling approach for estimating the joint angles of the index, middle fingers and the thumb.

D. Dynamic Neural networks (DNN)

We used DNN to estimate finger and thumb joint angle values. DNN, unlike static (feed-forward) neural networks, has a recurrent network structure and memory on the way from input to output which makes it a great candidate to estimate patterns in a time series and sequential data [31].

A Dynamic Neural Network with 1 sigmoid hidden layer, 2 delays and 1 linear output layer is used to estimate the joint angles shown in (Figure 1). First, we estimate the joint angles by using IMU sensors placed on the two finger and thumb phalanges (Figure 3, b), followed by an estimation of the same joint angles using the palm shape. Information from both DNNs is then fused to reach a higher precision of joint angle values.

E. Principal Component Analysis (PCA)

The high-dimensional pose features usually require the use of dimensionality reduction methods to make them computationally feasible. In this stage, we transform the input features to other values that are linearly uncorrelated, before applying them to the network. PCA method is used here to find principal components that have the largest possible variance and are orthogonal to each other. We performed mean centering and normalizing as prerequisites of PCA.

Each sensor produces 4 values ($q = [q_x, q_y, q_z, q_w]$). We use two sensors to estimate each joint, each of which has 4

values in experiments 1 and 2 which creates 8 features as input to the neural network. We include 95% of the information in the principal components, which can be achieved using 4 components of PCA. These components are used by two neural networks to estimate the joint angles from the palm measurements and the digit joint measurements, respectively. Finally, the output of each of the two networks, which are 3+3 values, are given to a third network to fuse the estimates and improve the accuracy of the results.

V. RESULTS AND DISCUSSION

Two different approaches have been investigated in order to improve the accuracy of the joint angle estimation: Normal sensor fusion, and Neural Network (DNN)-based sensor fusion.

A. Normal sensor fusion

In this approach, we use different combination of quaternion values of the palm and the digits as input to the neural network and calculate the accuracy (see Table III). Experiments details are:

- **Exp1:** raw quaternion values of the desired sensors over the joint as inputs of NN
- **Exp2:** raw quaternion values of the desired sensors over the palm as inputs of NN
- **Exp3:** raw quaternion values of the both inputs in exp1 & exp2 as inputs of NN
- **Exp3.A:** normal averaging the output values of the both exp1 & exp2
- **Exp3.B:** weighted averaging the output values of the both exp1 & exp2

The percentage error is calculated as:

$$\text{percentage_error} = \frac{\text{average_error} * 100}{\text{range}} \quad (1)$$

Table III demonstrates that averaging the estimation obtained in the experiments 1 and 2 can lead to a slightly better performance (exp3A & exp3B) as compared to using all the inputs to train a new model (Exp3). This can be partly caused by over fitting the network in Exp3. Averaging the two estimations gives better results than the experiments 1 and 2 independently except in the experiment 2 where the middle finger has 3.18% of average error, while standard and weighted average has 3.24% and 3.35% of average error, respectively.

B. PCA and NN based sensor fusion

In the second approach, PCA is used to reduce dimensionality of the raw quaternion values before sending them to neural network. In addition, in exp3 another neural network is used to combine results of exp 1 & 2. Therefore the experiment details are:

- **Exp1:** PCA values of the desired sensors over the joint as inputs of NN
- **Exp2:** PCA values of the desired sensors over the palm as inputs of NN

TABLE III
COMPARISON OF THE PERCENTAGE ERROR OF MODELS OBTAINED WITH IMU SENSOR (QUATERNIONS) DATA AS INPUT AND EULER ANGLES AS OUTPUT, IN EXPERIMENTS 1, 2 AND 3. (WITHOUT PCA)

Middle Finger					
Angle	Exp 1	Exp 2	Exp 3	Exp 3.A	Exp 3.B
Yaw	3.30%	2.02%	3.07%	2.64%	2.75%
Pitch	3.71%	4.16%	4.26%	3.34%	3.39%
Roll	4.82%	3.37%	3.80%	3.37%	3.93%
Average	3.94%	3.18%	3.71%	3.24%	3.35%
Index Finger					
Angle	Exp 1	Exp 2	Exp 3	Exp 3.A	Exp 3.B
Yaw	2.87%	2.57%	3.02%	2.53%	2.51%
Pitch	3.61%	3.51%	3.47%	3.34%	3.34%
Roll	2.96%	3.12%	2.97%	2.83%	2.85%
Average	3.14%	3.06%	3.15%	2.90%	2.90%
Thumb					
Angle	Exp 1	Exp 2	Exp 3	Exp 3.A	Exp 3.B
Yaw	3.41%	3.67%	5.76%	2.64%	2.69%
Pitch	4.27%	3.72%	3.19%	3.27%	3.38%
Roll	3.83%	2.74%	4.42%	3.00%	3.16%
Average	3.83%	3.37%	4.45%	2.97%	3.08%

* exp 3.A & 3.B show results of averaging and weighted averaging the results of exp 1 & 2 to acquire the joint angles.

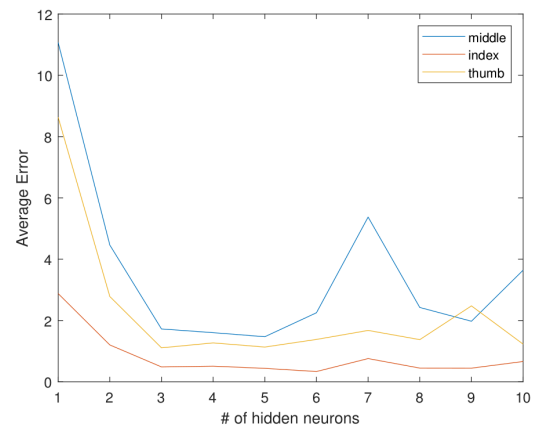


Fig. 5. General results of each finger with different number of neuron in the hidden layer

- **Exp3:** PCA values of the both inputs in exp1 & exp2 as inputs of NN

Table IV shows results of this method.

Combining the results of the first two experiments in the third NN shows somewhat improved performance when compared with the results from tracking fingers and thumb poses only or only palm shape poses (see Table IV). Figure 6 shows the comparison between the estimation and the ground truth of the thumb model. The response of the index and middle fingers have similar characteristics.

Fig. 5 shows variation of the average error for each digit against number of the neurons in the hidden layer. The error is calculated as the average of absolute value of the difference between the target and the estimation.

In general, the response of the index finger model is very much in line with the target. However, the discrepancy between the two is more obvious for small movements which

TABLE IV

COMPARISON OF PERCENTAGE ERROR OF MODELS OBTAINED WITH IMU SENSOR (QUATERNIONS) DATA AS INPUT AND EULER ANGLES AS OUTPUT, IN EXPERIMENTS 1, 2 AND 3.(WITH PCA)

Angle	Middle			Index			Thumb		
	Exp 1	Exp 2	Exp 3	Exp 1	Exp 2	Exp 3	Exp 1	Exp 2	Exp 3
Yaw	2.62%	2.57%	2.04%	3.50%	2.96%	2.98%	3.84%	3.94%	2.98%
Pitch	3.29%	2.91%	2.94%	3.85%	3.87%	3.81%	3.03%	3.30%	2.68%
Roll	2.61%	2.41%	2.44%	3.87%	3.72%	3.61%	4.16%	4.98%	1.70%
Average	2.84%	2.63%	2.47%	3.74%	3.52%	3.47%	3.68%	4.07%	2.45%

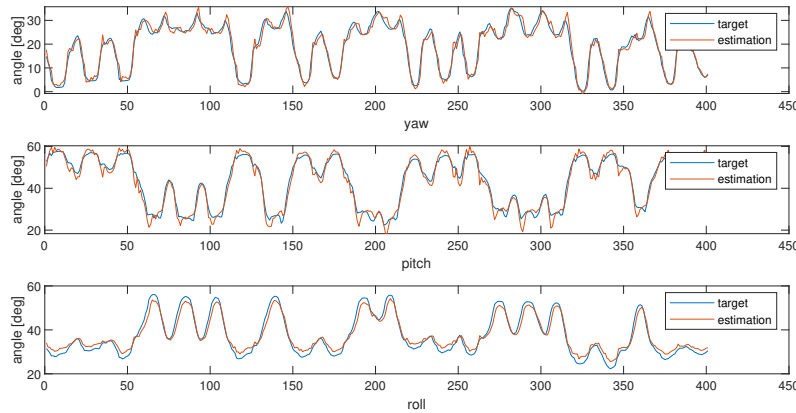


Fig. 6. Estimation of Yaw, Pitch and Roll values compared with the target

could be due to the generalization in the learning process. Furthermore, errors occur during fast changes in the movement direction. This can be observed in the peaks of the graph correspondent to the roll angle.

According to the experimental results tested on the validation data, using PCA to reduce the dimension of the input features (from palm and digits sensors), and fusing them using another neural network can lead to higher accuracy in the joint angle estimation.

VI. CONCLUSION

This paper proposed the possibility of using palm shape deformation in predicting the hand joint angles. IMU sensors over the palm and finger joints are used to obtain orientations of palm sections, as well as finger and thumb links. Supervised machine learning algorithms have been used to obtain the best possible models to interpret the sensors data. The DNN estimations have been compared with the ground truth obtained by the optical tracking system Polaris Spectra, and performance analysis of each model has been conducted.

The evidence from this study suggests that palm deformations positively contribute to better estimate kinematics of the hand and can improve gesture estimation accuracy. Thumb with 5-DOFs, is known to be a difficult structure to estimate, but since thumb is the principal component in deformation of the palm, taking this deformation into account simplifies thumb pose estimation process. These results contribute to the difficulty of accurate hand pose tracking in various application domains including human-robot interaction.

Our future work will focus on investigating more sophisticated machine learning methods in order to better estimate, not only the joint angles, but also the fingertips in a wider range of hand poses and grasp configurations. Further studies will also include an extensive testing of hand tracking evaluation in robotic tele-operation scenarios to test more intuitive and dexterous tele-manipulation.

REFERENCES

- [1] T. Feix, J. Romero, H.-B. Schmiemayer, A. M. Dollar, and D. Kragic, "The GRASP Taxonomy of Human Grasp Types," *IEEE Trans. Human-Machine Syst.*, vol. 46, pp. 66–77, feb 2016.
- [2] N. Wheatland, Y. Wang, H. Song, M. Neff, V. Zordan, and S. Jörg, "State of the art in hand and finger modeling and animation," in *Computer Graphics Forum*, vol. 34, pp. 735–760, Wiley Online Library, 2015.
- [3] F. P. van der Hulst, S. Schätzle, C. Preusche, and A. Schiele, "A functional anatomy based kinematic human hand model with simple size adaptation," in *2012 IEEE International Conference on Robotics and Automation*, pp. 5123–5129, IEEE, 2012.
- [4] M. F. Sani, S. Abeywardena, E. Psomopoulou, R. Ascione, and S. Dogramadzi, "Towards finger motion tracking and analyses for cardiac surgery,"
- [5] S. Saif, S. Tehseen, and S. Kausar, "A survey of the techniques for the identification and classification of human actions from visual data," *Sensors*, vol. 18, no. 11, p. 3979, 2018.
- [6] F.-Y. Liang, C.-H. Zhong, X. Zhao, D. L. Castro, B. Chen, F. Gao, and W.-H. Liao, "Online adaptive and lstm-based trajectory generation of lower limb exoskeletons for stroke rehabilitation," in *2018 IEEE International Conference on Robotics and Biomimetics (ROBIO)*, pp. 27–32, IEEE, 2018.
- [7] B. Doosti, "Hand pose estimation: A survey," *arXiv preprint arXiv:1903.01013*, 2019.
- [8] M. Bataineh, T. Marler, K. Abdel-Malek, and J. Arora, "Neural network for dynamic human motion prediction," *Expert Systems with Applications*, vol. 48, pp. 26–34, 2016.

- [9] Y. Cheng, W. Zhao, C. Liu, and M. Tomizuka, "Human motion prediction using adaptable neural networks," *arXiv preprint arXiv:1810.00781*, 2018.
- [10] N. Neverova, *Deep learning for human motion analysis*. PhD thesis, 2016.
- [11] J. Martinez, M. J. Black, and J. Romero, "On human motion prediction using recurrent neural networks," in *Proceedings of the IEEE Conference on Computer Vision and Pattern Recognition*, pp. 2891–2900, 2017.
- [12] B. Lang, "Oculus Claims Breakthrough in Hand-tracking Accuracy," 2018.
- [13] Plexus, "High-performance VR/AR Gloves," 2019.
- [14] HaptX, "Haptic gloves for VR training, simulation, and design," 2019.
- [15] A. P. Sangole and M. F. Levin, "Arches of the hand in reach to grasp," *J. Biomech.*, vol. 41, no. 4, pp. 829–837, 2008.
- [16] D. S. Richards, I. Georgilas, G. Dagnino, and S. Dogramadzi, "Powered exoskeleton with palm degrees of freedom for hand rehabilitation," *Proc. Annu. Int. Conf. IEEE Eng. Med. Biol. Soc. EMBS*, vol. 2015-Novem, pp. 4635–4638, 2015.
- [17] Y. Sugiura, F. Nakamura, W. Kawai, T. Kikuchi, and M. Sugimoto, "Behind the palm: Hand gesture recognition through measuring skin deformation on back of hand by using optical sensors," *2017 56th Annu. Conf. Soc. Instrum. Control Eng. Japan, SICE 2017*, vol. 2017-Novem, pp. 1082–1087, 2017.
- [18] R. Augustauskas and A. Lipnickas, "Robust hand detection using arm segmentation from depth data and static palm gesture recognition," in *2017 9th IEEE Int. Conf. Intell. Data Acquis. Adv. Comput. Syst. Technol. Appl.*, pp. 664–667, IEEE, sep 2017.
- [19] B. P. Nguyen, W.-L. Tay, and C.-K. Chui, "Robust Biometric Recognition From Palm Depth Images for Gloved Hands," *IEEE Trans. Human-Machine Syst.*, vol. 45, pp. 799–804, dec 2015.
- [20] A. Kumar and D. Zhang, "Personal recognition using hand shape and texture," *IEEE Trans. Image Process.*, vol. 15, pp. 2454–2461, aug 2006.
- [21] B. Zhang, W. Li, P. Qing, and D. Zhang, "Palm-Print Classification by Global Features," *IEEE Trans. Syst. Man, Cybern. Syst.*, vol. 43, pp. 370–378, mar 2013.
- [22] A. Gustus, G. Stillfried, J. Visser, H. Jörntell, and P. van der Smagt, "Human hand modelling: kinematics, dynamics, applications," *Biol. Cybern.*, vol. 106, no. 11-12, pp. 741–755, 2012.
- [23] A. Aranceta-Garza, H. Lakany, and B. Conway, "An Investigation into Thumb Rotation Using High Density Surface Electromyography of Extrinsic Hand Muscles," in *2013 IEEE Int. Conf. Syst. Man, Cybern.*, pp. 3751–3755, IEEE, oct 2013.
- [24] P. Aubin, K. Petersen, H. Sallum, C. Walsh, A. Correia, and L. Stirling, "A pediatric robotic thumb exoskeleton for at-home rehabilitation: The isolated orthosis for thumb actuation (IOTA)," *Int. J. Intell. Comput. Cybern.*, vol. 7, no. 3, pp. 233–252, 2014.
- [25] D. H. Kim and H.-S. Park, "Thumb joint angle estimation for soft wearable hand robotic devices," aug 2015.
- [26] E. Todorov and Z. Ghahramani, "Analysis of the synergies underlying complex hand manipulation," *26th Annu. Int. Conf. IEEE Eng. Med. Biol. Soc.*, vol. 2, pp. 4637–4640, 2005.
- [27] N. Polaris, "Northern digital polaris tracking system," 2004.
- [28] A. Deguet, R. Kumar, R. Taylor, and P. Kazanzides, "The cisst libraries for computer assisted intervention systems," in *MICCAI Workshop on Systems and Arch. for Computer Assisted Interventions, Midas Journal*, vol. 71, 2008.
- [29] Bosch Sensortec, "BNO055 Intelligent 9-axis absolute orientation sensor," tech. rep., 2014.
- [30] T. Instruments, "Pca9548a low-voltage 8-channel i2c switch with reset," 2015.
- [31] Matlab, "Introduction to dynamic neural networks."